

Optimality Deviation using the Koopman Operator [★]

Yicheng Lin ^{*} Bingxian Wu ^{*} Nan Bai ^{**} Yunxiao Ren ^{***}
 Zhisheng Duan ^{*}

^{*} School of Advanced Manufacturing and Robotics, Peking University, Beijing, 100871 China (e-mail: linyc020709@stu.pku.edu.cn, davidwu2003@stu.pku.edu.cn, duanzs@pku.edu.cn).

^{**} Department of Electronic and Computer Engineering, The Hong Kong University of Science and Technology, Hong Kong SAR, 999077 China (e-mail: eenanbai@ust.hk).

^{***} College of Engineering, Peking University, Beijing, 100871 China (e-mail: renyx@pku.edu.cn).

Abstract: This paper investigates the impact of approximation error in data-driven optimal control problem of nonlinear systems while using the Koopman operator. While the Koopman operator enables a simplified representation of nonlinear dynamics through a lifted state space, the presence of approximation error inevitably leads to deviations in the computed optimal controller and the resulting value function. We derive explicit upper bounds for these optimality deviations, which characterize the worst-case effect of approximation error. Supported by numerical examples, these theoretical findings provide a quantitative foundation for improving the robustness of data-driven optimal controller design.

Keywords: Data-driven control theory, nonlinear systems, robustness analysis, optimal control theory, Koopman operator.

1. INTRODUCTION

The Koopman operator has emerged as a powerful tool for analyzing nonlinear dynamical systems by transforming the state evolution into a simple representation in an infinite-dimensional space of observables (Koopman (1931)). In particular, it can be rigorously proved that the linear Koopman operator is able to transform finite-dimensional nonlinear autonomous systems without control input into infinite-dimensional linear ones (Korda and Mezić (2020)). For control-affine nonlinear systems, the Koopman operator enables transformation into bilinear form under mild assumptions (Goswami and Paley (2022)). This has inspired researchers to apply the well-established control theory of linear or bilinear systems to investigate the nonlinear system control problems, e.g., stability analysis (Mauroy and Mezić (2013, 2016)), feedback stabilization (Fu and You (2022); Lin et al. (2025)) and optimization (Vaidya (2025); Villanueva et al. (2021)).

Meanwhile, researchers have discovered the outstanding potential of the Koopman operator in data-driven control settings and also made some beneficial explorations theoretically as well as practically (Zhan et al. (2024), Pan et al. (2024)). In practical data-driven implementations using the Koopman operator, the system dynamics are often identified with a finite set of dictionary functions, for example using the well-known (extended) dynamic mode

decomposition (DMD/EDMD) algorithm and its variants (Korda and Mezić (2017)), then for the subsequent optimal control tasks, for example using learning based method (Caldarelli et al. (2025); Krolicki et al. (2022)) or model predictive control (MPC, Korda and Mezić (2018); Mamakoukas et al. (2022)).

However, the system identification procedure in data-driven control settings inevitably results in the approximation error, which can be mainly classified into projection error due to the finite-dimensional lifting, and estimation error due to limited data. Even though in model-based control settings using the Koopman operator, the projection error due to the finite-dimensional lifting still exists. This inevitably affects our interested control problems such like stabilization and optimization. Recent years have witnessed some progress in investigating the approximation error. For instance, Strässer et al. (2025, 2024) probabilistically or deterministically bound the error under certain assumptions and consider the feedback stabilization problem taking the error into account. In Mamakoukas et al. (2022); Zhang et al. (2022), robust Koopman-based MPC (r-KMPC or RK-MPC) is developed to deal with effects of the approximation error on constraint satisfaction or stability robustness.

Nevertheless, when an optimal controller is designed based on data and corresponding identified system without accounting for the approximation error, the actual closed-loop performance may deviate significantly from the theoretical optimum. Theoretically quantifying this deviation is crucial for ensuring performance robustness and reliabil-

[★] Financial support from the National Natural Science Foundation of China (NSFC) under grants T2121002, U24A20266 and 62173006 is greatly appreciated.

ity of the calculated controller in real-world applications, yet to the best of our knowledge, quantitative analysis of this optimality deviation remains largely unexplored.

In this paper, we address this gap by analyzing the optimality deviation caused by the approximation error in Koopman-based data-driven control. Specifically, we consider a control-affine nonlinear system and its bilinear lifted representation, where the approximation error is bounded proportionally to the state and input norms. We formulate an infinite-horizon optimal control problem with a quadratic cost and derive upper bounds for both deviations in the calculated optimal controller and value function without accounting for the approximation error between actual ones. Our analysis employs the Hamilton–Jacobi–Bellman (HJB) equation to capture the optimal controller and Hamilton–Jacobi–Isaacs (HJI) equation to capture the worst-case effect of the approximation error.

The main contributions of this work are as follows:

- *Theoretical Framework for Error Analysis:* We establish a systematic framework for analyzing optimality deviation due to the approximation error using the Koopman operator. It addresses a critical gap in the literature and provides a useful tool for analyzing other control methods, as detailed in Section 3.3.
- *Quantifiable Insights into Robustness:* Our derived upper bounds in Theorems 5 and 6 directly link the data-driven approximation error bound (coefficients c_1, c_2) to the degradation of optimal performance, offering crucial insights for designing robust controllers.
- *Empirical Verification:* Numerical experiments confirm that our theoretical bounds accurately capture performance deviations in a realistic nonlinear control scenario, which also show a promising direction to improve our controller design based on these analyses.

The remainder of this paper is organized as follows. Section 2 reviews the mathematical preliminaries of the Koopman operator and its use in system lifting. Section 3 presents the main theoretical results on optimality deviation analysis. Section 4 provides numerical examples, and Section 5 concludes the paper.

2. MATHEMATICAL PRELIMINARIES

Consider the unactuated nonlinear system

$$\dot{x}(t) = f(x(t)) \quad (1)$$

where $x \in \mathbb{R}^n$ denotes the state and $f(0) = 0$, i.e., the origin is an equilibrium of the unactuated system. We define a Banach space \mathcal{F} of observables $\varphi : \mathbb{R}^n \rightarrow \mathbb{R}$, and the Koopman operator is defined as follows.

Definition 1. The continuous time Koopman operator $\mathcal{K} : \mathcal{F} \rightarrow \mathcal{F}$ is defined as

$$(\mathcal{K}^t \varphi)(x_0) = \varphi \circ S(t, x_0) \quad (2)$$

where \circ denotes the function composition and $S(t, x_0)$ denotes the flow map (solution) of system (1) at time $t > 0$ with an initial state x_0 . Furthermore, under the assumption that $\varphi(x)$ is continuously differentiable, it satisfies

$$\frac{d\varphi(x)}{dt} = \mathcal{L}_f \varphi \triangleq \lim_{t \rightarrow 0} \frac{(\mathcal{K}^t \varphi - \varphi)}{t} = \nabla \varphi \cdot f \quad (3)$$

where \mathcal{L}_f is defined as the infinitesimal generator, also equals to the Lie derivative with respect to f .

We note that $\mathcal{K}^t(\alpha \varphi_1 + \beta \varphi_2) = \alpha \mathcal{K}^t \varphi_1 + \beta \mathcal{K}^t \varphi_2$, which indicates the linearity of Koopman operator even if the dynamics is nonlinear. This linearity naturally leads to the spectrum property, characterized by the Koopman eigenvalues and eigenfunctions.

Definition 2. A Koopman eigenfunction corresponding to the unactuated system (1) is an observable $\phi_\lambda \in \mathcal{F}$ such that

$$\mathcal{K}^t \phi_\lambda = e^{\lambda t} \phi_\lambda \quad (4)$$

for some $\lambda \in \mathbb{C}$, which is the associated Koopman eigenvalue. Additionally with (3), we obtain the following property of eigenfunctions

$$\mathcal{L}_f \phi_\lambda = \nabla \phi_\lambda \cdot f = \lambda \phi_\lambda. \quad (5)$$

It is known that if $\phi_{\lambda_1}, \phi_{\lambda_2}$ are Koopman eigenfunctions with eigenvalues λ_1, λ_2 respectively, $\phi_{\lambda_1}^{k_1} \phi_{\lambda_2}^{k_2}$ is also an eigenfunction with eigenvalue $k_1 \lambda_1 + k_2 \lambda_2$, which means that there are perhaps infinitely many eigenfunctions.

The Koopman eigenvalues and eigenfunctions play important roles in nonlinear system representation via the Koopman operator. Define a set of dictionary function $\Psi(x) = [\psi_1(x) \cdots \psi_N(x)]^\top \in \mathbb{R}^N$ serving as the transformation function. In order to completely capture nonlinear dynamics, $N > n$ is the usual case, so the system after transformation is often called lifted system. If a set of Koopman eigenfunctions $\Phi(x) = [\phi_{\lambda_1}(x) \cdots \phi_{\lambda_N}(x)]^\top$ are chosen to be the dictionary, (1) is transformed into a totally linear system

$$\frac{d}{dt} \Phi(x) = \Lambda \Phi(x) \quad (6)$$

where $\Lambda = \text{diag}(\lambda_1, \dots, \lambda_N)$. It is simple to prove that if the selected dictionary $\Psi(x)$ is equivalent to $\Phi(x)$, i.e., $\exists T \in \mathbb{R}^{N \times N}$, s.t. $\Psi(x) = T \Phi(x)$ with matrix T being full rank, the lifted system is also linear.

Certainly, besides relying on Koopman eigenfunctions, dictionary functions can be selected with different methods, for example, adopting various polynomials (Zhan et al. (2024)), or more complicated kernels (Strässer et al. (2024)). Without loss of generality, the following assumptions on $\Psi(x)$ are often adopted (Korda and Mezić (2018); Zhang et al. (2022)).

Assumption 3. The chosen dictionary functions satisfy

- (a) $\{\psi_i\}_{i=1}^N$ are continuously differentiable, and naturally $\Psi(x)$ is Lipschitz continuous with Lipschitz constant L_p .
- (b) $\Psi(0) = 0, \Psi^{-1}(0) = \{0\}$.
- (c) $\exists C \in \mathbb{R}^{N \times N}$, s.t. $x = C \Psi(x) = Cz$.

Now we consider the control-affine nonlinear system

$$\dot{x}(t) = f(x(t)) + \sum_{i=1}^m g_i(x(t)) u_i(t) \quad (7)$$

where $x \in \mathbb{R}^n, u = [u_1 \cdots u_m]^\top \in \mathbb{R}^m$ are the state and input respectively. Functions $f, g_i, i = 1, \dots, m$ are assumed to be continuously differentiable. The nonlinear system (7) can be simplified via the Koopman operator for the convenience of research. In particular, the time derivative of the chosen dictionary $\Psi(x)$ is

$$\frac{d\Psi}{dt} = \frac{\partial\Psi}{\partial x}f(x) + \sum_{i=1}^m u_i \frac{\partial\Psi}{\partial x}g_i(x) = \mathcal{L}_f\Psi + \sum_{i=1}^m u_i \mathcal{L}_{g_i}\Psi. \quad (8)$$

As shown in Goswami and Paley (2022), if the eigenspace of \mathcal{L}_f is an invariant subspace of \mathcal{L}_{g_i} , $i = 1, \dots, m$, system (8) (hence (7)) is bilinearizable. If this is not satisfied, a projection error term can be introduced such that

$$\frac{dz}{dt} = Az + B_0u + \sum_{i=1}^m u_i B_i z + r(z, u). \quad (9)$$

In data-driven control settings, matrices A , B_0 and B_i , $i = 1, \dots, m$ are identified from data, and not only projection error but also estimation error resulting from finite data are contained in $r(z, u)$. Specific methodologies are not discussed in detail as they are not the main focus of this paper. However, the proportional bound of approximation error $r(z, u)$ given by the following assumption possesses a certain degree of universality.

Assumption 4. Suppose there exist constants $c_1, c_2 > 0$ such that the approximation error term in (9), including projection error and estimation error, is bounded by

$$\|r(z, u)\| \leq c_1\|z\| + c_2\|u\|. \quad (10)$$

Furthermore, the partial derivative $\frac{\partial r}{\partial u}$ is assumed to exist and be continuous.

Note that the error bound has been investigated in several recent papers which indicates that Assumption 4 is not strong and is also the truth in a large number of cases. For instance, a probabilistic bound for the estimation error $c_1, c_2 \in \mathcal{O}(1/\sqrt{\delta d_0})$ is derived (Strässer et al., 2024, Proposition 5), where $\mathcal{O}(\cdot)$ is the Big O notation, δ and d_0 denote the probability tolerance and data amount respectively. Leveraging kernel-based methods, deterministic bound for the approximation error was established (Strässer et al., 2025, Theorem 5). These results ensure the correctness of proportional error bound relationship (10). In fact, the approximation error term can be represented by

$$r(z, u) = \mathcal{L}_f\Psi - A\Psi + \sum_{i=1}^m u_i (\mathcal{L}_{g_i}\Psi - B_{0,i} - B_i\Psi) \quad (11)$$

where $B_{0,i}$ denotes the i -th column of B_0 , then

$$\frac{\partial r}{\partial u} = \sum_{i=1}^m (\mathcal{L}_{g_i}\Psi - B_{0,i} - B_i\Psi) e_i \quad (12)$$

where e_i denotes the unit vector with the i -th component being 1. This illustrate the continuous differentiability of $r(z, u)$ with respect to u .

3. OPTIMALITY DEVIATION ANALYSIS

The main focus of this paper is the deviation of data-driven optimal controller design using the Koopman operator. Consider the following infinite-horizon optimal control problem under quadratic performance index, i.e.,

$$\min_{u(\cdot)} J(u(\cdot)) = \int_0^\infty \frac{1}{2} [x^\top(t) \bar{Q} x(t) + u^\top(t) R u(t)] dt \quad (13)$$

where $\bar{Q} \succ 0$, $R \succ 0$. A common scenario in data-driven control applications is that one has no exact knowledge of the approximation error term $r(z, u)$, making it challenging to design the optimal controller for the actual bilinear system (9) that takes the error into consideration, and

equivalently for the original nonlinear system (7). Under this circumstance, an ideal approach is to calculate the optimal controller for (9) without considering the error, i.e.,

$$\begin{aligned} V_0^*(z) &= \min_{u(\cdot)} \int_0^\infty \frac{1}{2} [z^\top(t) Q z(t) + u^\top(t) R u(t)] dt \\ \text{s.t. } \dot{z}(t) &= Az(t) + B(z(t))u(t), \quad z(0) = z \end{aligned} \quad (14)$$

where for ease of representation we denote

$$Q = C^\top \bar{Q} C, \quad B(z) = B_0 + \sum_{i=1}^m B_i z e_i^\top. \quad (15)$$

With the well-known HJB equation (Aganovi and Gaji (1995)), the optimal value function $V_0^*(z)$ is calculated with

$$(\nabla V_0^*)^\top A z + \frac{1}{2} z^\top Q z - \frac{1}{2} (\nabla V_0^*)^\top B(z) R^{-1} B^\top(z) \nabla V_0^* = 0. \quad (16)$$

leading to the calculated optimal controller

$$u_0^*(z) = -R^{-1} B^\top(z) \nabla V_0^*. \quad (17)$$

There exist a considerable number of works on solving the optimal control problem for bilinear systems (Aganovi and Gaji (1995); Halperin (2023)) although it is not a simple task. Further developing suitable and efficient bilinear optimal control methods is also a promising direction for Koopman-based data-driven optimal control. However, the actual system dynamics (9) contains the approximation error term. Consequently, no matter how advanced the calculation method is, applying u_0^* to the actual system will result in performance deviation, which will be analyzed in the following text.

3.1 Deviation of Optimal Value Function

First, we consider the deviation between the actual optimal value function and calculated one $V_0^*(z)$ starting with the following theorem.

Theorem 5. Due to the existence of approximation error, the calculated optimal controller u_0^* given by (16) and (17) results in an extra cost compared with V_0^* , characterized by

$$\begin{aligned} \|V - V_0^*\| &\leq \Delta V_{\max} \\ &= \max \left\{ \frac{2c_1 L_p}{\sqrt{\lambda_{\min}(\bar{Q})}}, \frac{2c_2}{\sqrt{\lambda_{\min}(R)}} \right\} \left(V_0^* \int_0^\infty \|\nabla V_0^*\|^2 dt \right)^{\frac{1}{2}} \end{aligned} \quad (18)$$

where $V(z)$ denotes the value function that corresponds to the closed-loop system (7) controlled by $u_0^*(z)$.

Proof. Here we use the notation $J(u, z, r)$ since J is actually a function of the initial state $z(0) = z$, the control input $u(t)$ and the approximation error term $r(z(t), u(t))$. Apparently $V_0^*(z) = J(u_0^*, z, 0)$, and we denote $V(z) = J(u_0^*, z, r)$. In addition, we define a set \mathcal{R} whose elements are all the possible forms of the approximation error satisfying (10), i.e.,

$$\mathcal{R} = \{r(z, u) | \|r(z, u)\| \leq c_1\|z\| + c_2\|u\|\}. \quad (19)$$

In order to bound $V - V_0^*$, we firstly investigate the worst-case error $r_0^* = \arg \max_{r \in \mathcal{R}} J(u_0^*, z, r)$ that tries to maximize the quadratic value function. Using the HJI

equation (Aliyu (2011)), the worst-case error r_0^* should be solved from

$$\begin{aligned} \max_{r \in \mathcal{R}} \{ & (\nabla V_r^*)^\top [Az + B(z)u_0^* + r(z, u_0^*)] \\ & + \frac{1}{2}z^\top Qz + \frac{1}{2}(u_0^*)^\top Ru_0^* \} = 0, \end{aligned} \quad (20)$$

therefore satisfies

$$r_0^* = \frac{c_1\|z\| + c_2\|u_0^*\|}{\|\nabla V_r^*\|} \nabla V_r^* \quad (21)$$

where $V_r^*(z) = J(u_0^*, z, r_0^*)$ is the solution of

$$\begin{aligned} & (\nabla V_r^*)^\top Az + \frac{1}{2}z^\top Qz + (c_1\|z\| + c_2\|u_0^*\|)\|\nabla V_r^*\| \\ & + \frac{1}{2}(\nabla V_0^*)^\top B(z)R^{-1}B^\top(z)\nabla V_0^* \\ & - (\nabla V_r^*)^\top B(z)R^{-1}B^\top(z)\nabla V_0^* = 0. \end{aligned} \quad (22)$$

The time derivative of $V_r^* - V_0^*$ is the inner product of its gradient and \dot{z} , thus satisfying

$$\frac{d}{dt}(V_r^* - V_0^*) = -\nabla(V_0^*)^\top \frac{c_1\|z\| + c_2\|u_0^*\|}{\|\nabla V_r^*\|} \nabla V_r^* \quad (23)$$

which is obtained with (16) and (22), then

$$\left\| \frac{d}{dt}(V^* - V_0^*) \right\| \leq \|\nabla V_0^*\| (c_1\|z\| + c_2\|u_0^*\|). \quad (24)$$

With the bound of time derivative of $V_r^* - V_0^*$, we obtain

$$\begin{aligned} \|V_r^* - V_0^*\| & \leq \int_0^\infty \left\| \frac{d}{dt}(V_r^* - V_0^*) \right\| dt \\ & \leq \left(\int_0^\infty \|\nabla V_0^*\|^2 dt \right)^{\frac{1}{2}} \left(\int_0^\infty (c_1\|z\| + c_2\|u_0^*\|)^2 dt \right)^{\frac{1}{2}}. \end{aligned} \quad (25)$$

The last integral term corresponding to the approximation error can be bounded by

$$\begin{aligned} & \int_0^\infty (c_1\|z\| + c_2\|u_0^*\|)^2 dt \\ & = \int_0^\infty (c_1^2\|z\|^2 + 2c_1c_2\|z\|\|u_0^*\| + c_2^2\|u_0^*\|^2) dt \\ & \leq \int_0^\infty 2(c_1^2\|z\|^2 + c_2^2\|u_0^*\|^2) dt \\ & \leq \int_0^\infty 2(c_1^2L_p^2\|x\|^2 + c_2^2\|u_0^*\|^2) dt. \end{aligned} \quad (26)$$

With the inequalities

$$\begin{aligned} \lambda_{\min}(\bar{Q})\|x\|^2 & \leq x^\top \bar{Q}x \leq \lambda_{\max}(\bar{Q})\|x\|^2, \\ \lambda_{\min}(R)\|u\|^2 & \leq u^\top \bar{Q}u \leq \lambda_{\max}(R)\|u\|^2, \end{aligned} \quad (27)$$

and the fact that $x^\top \bar{Q}x = z^\top Qz$, we obtain

$$\begin{aligned} & \int_0^\infty 2(c_1^2L_p^2\|x\|^2 + c_2^2\|u_0^*\|^2) dt \\ & \leq \int_0^\infty \left(\frac{2c_1^2L_p^2}{\lambda_{\min}(\bar{Q})} x^\top \bar{Q}x + \frac{2c_2^2}{\lambda_{\min}(R)} (u_0^*)^\top Ru_0^* \right) dt \\ & \leq \max \left\{ \frac{4c_1^2L_p^2}{\lambda_{\min}(\bar{Q})}, \frac{4c_2^2}{\lambda_{\min}(R)} \right\} \int_0^\infty \frac{1}{2}[z^\top Qz + (u_0^*)^\top Ru_0^*] dt \\ & = \max \left\{ \frac{4c_1^2L_p^2}{\lambda_{\min}(\bar{Q})}, \frac{4c_2^2}{\lambda_{\min}(R)} \right\} V_0^*(z). \end{aligned} \quad (28)$$

Combining (25), (26) and (28) leads to (18). It is also likely that the approximation error term reduces the value

function. Specifically, $r_0^{**} = \arg \min_{r \in \mathcal{R}} J(u_0^*, z, r)$ should be solved from HJB equation

$$\begin{aligned} \min_{r \in \mathcal{R}} \{ & (\nabla V_r^{**})^\top [Az + B(z)u_0^* + r(z, u_0^*)] \\ & + \frac{1}{2}z^\top Qz + \frac{1}{2}(u_0^*)^\top Ru_0^* \} = 0, \end{aligned} \quad (29)$$

which leads to its form

$$r_0^{**} = -\frac{c_1\|z\| + c_2\|u_0^*\|}{\|\nabla V_r^{**}\|} \nabla V_r^{**}. \quad (30)$$

The time derivative can also be obtained

$$\frac{d}{dt}(V_r^{**} - V_0^*) = \nabla(V_0^*)^\top \frac{c_1\|z\| + c_2\|u_0^*\|}{\|\nabla V_r^{**}\|} \nabla V_r^{**} \quad (31)$$

and the same upper bound of $\|V_r^{**} - V_0^*\|$ can be with a similar way and leads to the same result with (18). The proof is completed. \square

3.2 Deviation of Optimal Controller

It is worth noticing that $V(z)$ in Theorem 5 is not the actual optimal value function corresponding to the actual system (9). Instead, it captures the extra cost when the calculated controller u_0^* is utilized, and the worst-case is captured by the upper bound ΔV_{\max} . However, analysis on $V(z)$ is the basis of that on the deviation between $u_0^*(z)$ and the actual optimal controller, as discussed in the following theorem.

Theorem 6. Due to the existence of approximation error, the calculated optimal controller u_0^* given by (16) and (17) deviates from the actual optimal controller u^* corresponding to the original nonlinear system (7). Specifically, this deviation is characterized by

$$\begin{aligned} & \int_0^\infty (u_0^* - u^*)^\top R(u_0^* - u^*) dt \\ & \leq 2\Delta V_{\max} \left[1 + \left(1 + \frac{\Delta V_{\max}}{V_0^*} \right)^{\frac{1}{2}} \right]. \end{aligned} \quad (32)$$

Proof. Denote V^* as the actual value function that corresponds to the closed-loop control-affine nonlinear system (7) with the actual optimal controller u^* , which should be solved from the following HJB equation

$$\min_u \left\{ \frac{\partial V^*}{\partial x} [f(x) + g(x)u] + \frac{1}{2}x^\top \bar{Q}x + \frac{1}{2}u^\top Ru \right\} = 0. \quad (33)$$

We remark that V^* and u^* are also functions of the lifted state since the relation $x = Cz$ exists, thus afterwards use notations $V^*(z)$, $u^*(z)$ and $\nabla V^* = \frac{\partial V^*}{\partial z}$ without loss of generality. Due to the equivalence of (8) and (9) under the existence of approximation error term $r(z, u)$, we obtain

$$\begin{aligned} \min_u \{ & (\nabla V^*)^\top [Az + B(z)u + r(z, u)] \\ & + \frac{1}{2}z^\top Qz + \frac{1}{2}u^\top Ru \} = 0. \end{aligned} \quad (34)$$

As the partial derivative of $r(z, u)$ with respect to u is assumed to exist, the actual optimal controller satisfies

$$u^*(z) = -R^{-1} \left(B(z) + \frac{\partial r}{\partial u}(z, u^*) \right)^\top \nabla V^*(z). \quad (35)$$

Also denote $r_{u^*} = \frac{\partial r}{\partial u}(z, u^*)$, and $V^*(z)$ is the solution of

$$\begin{aligned}
& (\nabla V^*)^\top A z + \frac{1}{2} z^\top Q z - \frac{1}{2} (\nabla V^*)^\top B(z) R^{-1} B^\top(z) \nabla V^* \\
& + (\nabla V^*)^\top r(z, u^*) + \frac{1}{2} (\nabla V^*)^\top r_{u^*} R^{-1} r_{u^*}^\top \nabla V^* = 0.
\end{aligned} \tag{36}$$

Combining (35) with (17) results in

$$u_0^* - u^* = R^{-1} B^\top(z) \nabla (V^* - V_0^*) + R^{-1} r_{u^*}^\top \nabla V^*, \tag{37}$$

then with (36) and (16) we obtain

$$\begin{aligned}
& (u_0^* - u^*)^\top R(u_0^* - u^*) = -2 (\nabla V_0^*)^\top r(z, u^*) \\
& - 2 \nabla (V^* - V_0^*)^\top [A z + B(z) u^* + r(z, u^*)].
\end{aligned} \tag{38}$$

We observe that the last term in (38) is actually the time derivative of $-(V^* - V_0^*)$ along the system trajectory controlled by the optimal controller u^* . By integrating along this trajectory we find that

$$\begin{aligned}
& \int_0^\infty (u_0^* - u^*)^\top R(u_0^* - u^*) dt \\
& = -2 \int_0^\infty \left[\frac{d}{dt} (V^* - V_0^*) + (\nabla V_0^*)^\top r(z(t), u^*(z(t))) \right] dt \\
& = 2(V^*(z) - V_0^*(z)) - 2 \int_0^\infty (\nabla V_0^*)^\top r(z(t), u^*(z(t))) dt
\end{aligned} \tag{39}$$

since we assume that the optimal controller stabilizes the system thus $V^*(z(\infty)) = V_0^*(z(\infty)) = 0$. Following similar procedures in (25), (26) and (28), we obtain

$$\begin{aligned}
& \left\| \int_0^\infty (\nabla V_0^*)^\top r(z(t), u^*(z(t))) dt \right\| \\
& \leq \left(\int_0^\infty \|\nabla V_0^*\|^2 dt \right)^{\frac{1}{2}} \left(\int_0^\infty (c_1 \|z\| + c_2 \|u^*\|)^2 dt \right)^{\frac{1}{2}} \\
& \leq \max \left\{ \frac{2c_1 L_p}{\sqrt{\lambda_{\min}(\bar{Q})}}, \frac{2c_2}{\sqrt{\lambda_{\min}(R)}} \right\} \left(V^* \int_0^\infty \|\nabla V_0^*\|^2 dt \right)^{\frac{1}{2}}.
\end{aligned} \tag{40}$$

Now we use the notation $J(u, z, r)$ once again (the same with proof of Theorem 5) to facilitate the following analysis. Apparently the relations

$$\begin{aligned}
V_r^*(z) &= J(u_0^*, z, r_0^*) \geq V(z) = J(u_0^*, z, r) \\
V_r^*(z) &= J(u_0^*, z, r_0^*) \geq V_0^*(z) = J(u_0^*, z, 0) \\
V(z) &= J(u_0^*, z, r) \geq V^*(z) = J(u^*, z, r)
\end{aligned} \tag{41}$$

hold. If $V^*(z) \geq V_0^*(z)$, we have

$$V^* - V_0^* = V^* - V + V - V_0^* \leq V - V_0^* \leq \Delta V_{\max}, \tag{42}$$

and obtain the following relation

$$V^* \leq V_0^* + \Delta V_{\max} \tag{43}$$

which naturally holds if $V^*(z) \leq V_0^*(z)$. Then inequalities (40) can be further processed, i.e.,

$$\begin{aligned}
& \left\| \int_0^\infty (\nabla V_0^*)^\top r(z(t), u^*(z(t))) dt \right\| \\
& \leq \frac{\Delta V_{\max}}{(V_0^*)^{\frac{1}{2}}} (V^*)^{\frac{1}{2}} \leq \Delta V_{\max} \left(1 + \frac{\Delta V_{\max}}{V_0^*} \right)^{\frac{1}{2}}.
\end{aligned} \tag{44}$$

Along with equation (39), the deviation of controller satisfies (32). The proof is completed. \square

The proof confirms that the deviation between V_0^* and the actual value function V^* also satisfies $V^* - V_0^* \leq \Delta V_{\max}$.

3.3 Discussion on the Theoretical Results

With the established results, we have analyzed the impact of approximation error in Koopman-based control methods on achieving optimality from a more comprehensive perspective.

Firstly, we make the abstract notion of optimality deviation concrete and computable. The bounds in Theorems 5 and 6 are explicitly parameterized by the error coefficients (c_1, c_2) and the calculated optimal value function V_0^* . This structure directly links the intrinsic error to the resulting performance loss, providing a pathway to estimate the deviation when the exact form of approximation error is unknown.

Additionally, our methodology can be regarded as a novel and general strategy for analyzing optimality deviations under various control methods. Directly linking the calculated optimal solution (16) and actual one (36) is intractable, hence we introduce the worst-case value function V_r^* as an analytical intermediary. This approach can be adapted to other data-driven control schemes, for example, the widely used Koopman-based linear optimal control methods (Korda and Mezić (2018, 2020)), which can be regarded as special cases of our methodology letting $B(z) = B_0$ in (16).

Finally, this analysis paves the way for robust controller design. There are several possible directions based on the established results which include, for instance, reducing the error with better system identification method, avoiding the worst-case optimality deviation, or adjusting the calculated controller towards the actual optimum. We will also fully utilize the established results in future work to improve the performance of designed controllers, which will further benefit practical applications.

4. NUMERICAL EXAMPLES

Consider the optimal control problem of the following control-affine nonlinear system

$$\begin{bmatrix} \dot{x}_1 \\ \dot{x}_2 \end{bmatrix} = \begin{bmatrix} -x_1 + x_2 \\ -\frac{1}{2}(x_1 + x_2) + \frac{1}{2}x_1^2 x_2 \end{bmatrix} + \begin{bmatrix} 0 \\ x_1 \end{bmatrix} u \tag{45}$$

where the weighting matrices in the quadratic index are set as $\bar{Q} = I_{2 \times 2}, R = 1$. We can verify the analytical solution (i.e. the optimal value function) of HJB equation for system (45) is $V^*(x) = \frac{1}{4}x_1^2 + \frac{1}{2}x_2^2$, which induces the optimal controller $u^*(x) = -x_1 x_2$.

In our simulation, the system dynamics (45) is only used for generating time-series data $\{x_j, \dot{x}_j\}_{j=1}^{N_t}$ collected from $N_t = 40$ trajectories with each length of $t = 1s$. The dictionary functions $\Psi(x)$ are constructed as polynomials up to order 4 of the state variable x , thus the Lipschitz constant L_p can be calculated. The adopted method for data-driven system identification is the most widely used algorithm EDMD, whose convergence has been proved in Korda and Mezić (2017) with applications on a variety of control problems including robots (Bruder et al. (2021)), quadrotors (Oh et al. (2024)), smart grids (Jiang et al. (2024)), etc. Despite the existence of its variants, fundamental methodology remains the same. We introduce the following matrices composed of the collected data, i.e.,

$$\begin{aligned}
U_0 &:= [u_1 \ u_2 \ \cdots \ u_T] \\
Z_0 &:= [z_1 \ z_2 \ \cdots \ z_T] \\
&= [\Psi(x_1) \ \Psi(x_2) \ \cdots \ \Psi(x_T)] \\
V_0^i &:= [u_1^i z_1 \ u_2^i z_2 \ \cdots \ u_T^i z_T] \\
Z_1 &:= [z_1 \ z_2 \ \cdots \ z_T] \\
&= [\nabla \Psi(x_1) \cdot \dot{x}_1 \ \nabla \Psi(x_2) \cdot \dot{x}_2 \ \cdots \ \nabla \Psi(x_T) \cdot \dot{x}_T]
\end{aligned} \tag{46}$$

where u_j^i , $i = 1, \dots, m$, $j = 1, 2, \dots, T$ denotes the i -th component of the control input u_j . Denote $W_0 = [Z_1^\top \ U_0^\top \ Z_1^\top \ \cdots \ Z_m^\top]^\top$, and EDMD algorithm solves the least square problem

$$\min_{A, B_0, B_1, \dots, B_m} \|Z_1 - [A \ B_0 \ B_1 \ \cdots \ B_m] W_0\| \tag{47}$$

which leads to the solution

$$[A \ B_0 \ B_1 \ \cdots \ B_m] = Z_1 W_0^\dagger \tag{48}$$

and identifies the bilinear system (9). Meanwhile, it is also feasible to determine the coefficients c_1, c_2 of error bound (10) from the collected data. Specifically, denote

$$R = [r_1 \ r_2 \ \cdots \ r_T] = Z_1 - [A \ B_0 \ B_1 \ \cdots \ B_m] W_0 \tag{49}$$

which records the error values at all the data points, and

$$\begin{aligned}
\tilde{R} &= [\|r_1\| \ \|r_2\| \ \cdots \ \|r_T\|], \tilde{Z}_0 = [\|z_1\| \ \|z_2\| \ \cdots \ \|z_T\|], \\
\tilde{U}_0 &= [\|u_1\| \ \|u_2\| \ \cdots \ \|u_T\|].
\end{aligned} \tag{50}$$

Then the coefficients are solved with constraints

$$\tilde{R} \leq c_1 \tilde{Z}_0 + c_2 \tilde{U}_0. \tag{51}$$

The main objective of our simulation is to verify the optimality deviation derived in Theorems 5 and 6, therefore we focus on $V^* - V_0^*$ where V_0^* is calculated using state-dependent algebraic Riccati equation (SDARE, Aganovi and Gaji (1995)). Specifically, sufficient initial points are selected within our interested region $\mathbb{X} = [-1, 1]^2$, and the optimal control problem together with u_0^*, V_0^* is solved with SDARE for each chosen initial point, then ∇V_0^* is also available for determining ΔV_{\max} . Simulation results are exhibited with Figs.1-3, confirming that ΔV_{\max} provides an accurate characterization for optimality deviation.

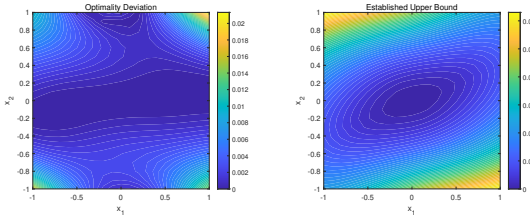


Fig. 1. Contour lines of optimality deviation $V^* - V_0^*$ and the upper bound ΔV_{\max} established by Theorem 5.

5. CONCLUSION

In this paper, we have presented a theoretical analysis of the optimality deviation in data-driven optimal control based on the Koopman operator. Our work addresses a critical, yet often overlooked, issue—the impact of inherent approximation error on the performance and optimality of the designed controllers. This analysis provides a theoretical foundation for understanding the sub-optimality gap and paves the way for robust controller synthesis.

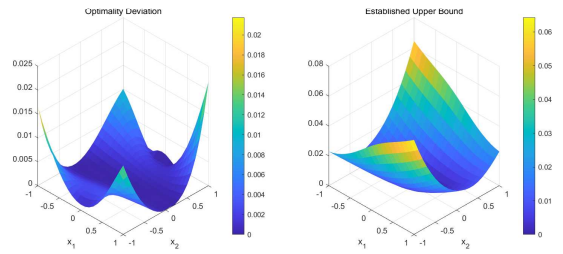


Fig. 2. 3D plots for optimality deviation $V^* - V_0^*$ and the established upper bound ΔV_{\max} .

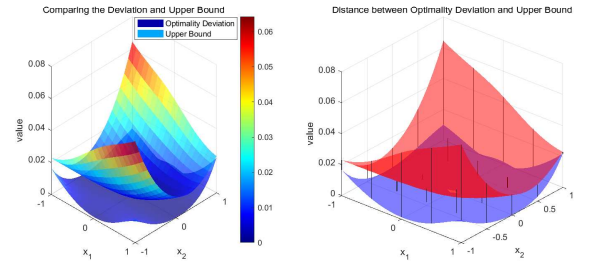


Fig. 3. Comparison of $V^* - V_0^*$ and ΔV_{\max} , which shows that ΔV_{\max} gives an ideal bound of $V^* - V_0^*$.

Future work will focus on several important directions. One immediate goal is to extend the analysis to output feedback or uncertain systems. Another promising direction is to leverage the derived optimality deviation for the development of robust or adaptive Koopman-based controllers that can actively compensate for model inaccuracies and move forward to the actual optimum. Finally, exploring more efficient system identification algorithms and more advanced bilinear control methods, e.g., Vaidya (2025); Villanueva et al. (2021), represents a fundamental path toward improving the reliability and efficiency of data-driven optimal control using the Koopman operator.

REFERENCES

- Aganovi, Z. and Gaji, Z. (1995). *Linear optimal control of bilinear systems with applications to singular perturbations and weak coupling*. Springer.
- Aliyu, M. (2011). *Nonlinear H-infinity-control, Hamiltonian systems and Hamilton-Jacobi equations*. CRC.
- Bruder, D., Fu, X., Gillespie, R.B., Remy, C.D., and Vasudevan, R. (2021). Data-driven control of soft robots using Koopman operator theory. *IEEE Transactions on Robotics*, 37(3), 948–961.
- Caldarelli, E., Chatalic, A., Colomé, A., Molinari, C., Ocampo-Martinez, C., Torras, C., and Rosasco, L. (2025). Linear quadratic control of nonlinear systems with Koopman operator learning and the Nyström method. *Automatica*, 177, 112302.
- Fu, X. and You, K. (2022). Direct data-driven stabilization of nonlinear affine systems via the Koopman operator. In *2022 IEEE 61st Conference on Decision and Control (CDC)*, 2668–2673.
- Goswami, D. and Paley, D.A. (2022). Bilinearization, reachability, and optimal control of control-affine nonlinear systems: A Koopman spectral approach. *IEEE Transactions on Automatic Control*, 67(6), 2715–2728.

Halperin, I. (2023). Solution of the continuous time bilinear quadratic regulator problem by Krotov's method. *IEEE Transactions on Automatic Control*, 68(4), 2415–2421.

Jiang, X., Li, Y., and Huang, D. (2024). Modularized bilinear Koopman operator for modeling and predicting transients of microgrids. *IEEE Transactions on Smart Grid*, 15(5), 5219–5231.

Koopman, B.O. (1931). Hamiltonian systems and transformation in Hilbert space. *Proceedings of the National Academy of Sciences*, 17(5), 315–318.

Korda, M. and Mezić, I. (2017). On convergence of extended dynamic mode decomposition to the Koopman operator. *Journal of Nonlinear Science*, 28(2), 687–710.

Korda, M. and Mezić, I. (2018). Linear predictors for nonlinear dynamical systems: Koopman operator meets model predictive control. *Automatica*, 93, 149–160.

Korda, M. and Mezić, I. (2020). Optimal construction of Koopman eigenfunctions for prediction and control. *IEEE Transactions on Automatic Control*, 65(12), 5114–5129.

Krolicki, A., Sutavani, S., and Vaidya, U. (2022). Koopman-based policy iteration for robust optimal control. In *2022 American Control Conference (ACC)*, 1317–1322.

Lin, Y., Wu, B., Bai, N., Sun, Z., Ren, Y., Chen, C., and Duan, Z. (2025). Integrating uncertainties for Koopman-based stabilization. *arXiv*, 2508.11533.

Mamakoukas, G., Di Cairano, S., and Vinod, A.P. (2022). Robust model predictive control with data-driven Koopman operators. In *2022 American Control Conference (ACC)*, 3885–3892.

Mauroy, A. and Mezić, I. (2013). A spectral operator-theoretic framework for global stability. In *52nd IEEE Conference on Decision and Control*, 5234–5239.

Mauroy, A. and Mezić, I. (2016). Global stability analysis using the eigenfunctions of the Koopman operator. *IEEE Transactions on Automatic Control*, 61(11), 3356–3369.

Oh, Y., Hoon Lee, M., and Moon, J. (2024). Koopman-based control system for quadrotors in noisy environments. *IEEE Access*, 12, 71675–71684.

Pan, J., Li, D., Wang, J., Zhang, P., Shao, J., and Yu, J. (2024). Autogeneration of mission-oriented robot controllers using Bayesian-based Koopman operator. *IEEE Transactions on Robotics*, 40, 903–918.

Strässer, R., Schaller, M., Berberich, J., Worthmann, K., and Allgöwer, F. (2025). Kernel-based error bounds of bilinear Koopman surrogate models for nonlinear data-driven control. *IEEE Control Systems Letters*, 9, 1892–1897.

Strässer, R., Schaller, M., Worthmann, K., Berberich, J., and Allgöwer, F. (2024). Koopman-based feedback design with stability guarantees. *IEEE Transactions on Automatic Control*, 1–16.

Vaidya, U. (2025). When Koopman meets Hamilton and Jacobi. *IEEE Transactions on Automatic Control*, 1–16.

Villanueva, M.E., Jones, C.N., and Houska, B. (2021). Towards global optimal control via Koopman lifts. *Automatica*, 132, 109610.

Zhan, W., Miao, Z., Zhang, H., Chen, Y., Wu, Z.G., He, W., and Wang, Y. (2024). Resilient formation control with Koopman operator for networked NMRs under denial-of-service attacks. *IEEE Transactions on Systems, Man, and Cybernetics: Systems*, 54(11), 7065–7078.

Zhang, X., Pan, W., Scattolini, R., Yu, S., and Xu, X. (2022). Robust tube-based model predictive control with Koopman operators. *Automatica*, 137, 110114.